Mechanical behavior of western alpine structures inferred from statistical analysis of seismicity

Christian Sue
Geological Institute, Neuchâtel University, Switzerland

Jean Robert Grasso
LGIT, Grenoble Observatory, France

Franz Lahaie
Department Geology, University College Dublin, Ireland

David Amitrano
LAEGO-EMN, Nancy, France

Received 7 September 2001; revised 18 January 2002; accepted 12 February 2002; published 24 April 2002.

[1] Two seismic arcs (150 km and 120 km long) located in the western Alps, 50 km apart from each other, are characterized by different statistical patterns in energy and space domains. For the two arcs, we found power-law distributions in energy domain with a lower b-value and fall-off for large events for the easternmost arc only, and roughly similar spatial damage. By comparing the shape and the statistical parameters of these distributions with those provided by numerical models of rock damage, we suggest a relatively more brittle behavior for one area with respect to the other. We discuss the implications of the observed distributions in terms of tectonics and of mechanics of faulting. We suggest three candidates to drive the relative changes in seismicity distribution between the two arcs: the earthquake depth, the host rock composition, and the inherited fracturing patterns. *INDEX TERMS:* 7209 Seismology: Earthquake dynamics and mechanics; 7230 Seismology: Seismicity and seismotectonics; 8010 Structural Geology: Fractures and faults

1. Introduction

[2] Seismicity maps the brittle damage of the upper crust. Statistical variations in seismicity patterns have been reported, both in terms of the frequency-size distribution of earthquakes [*Wiemer and Wyss*, 1997; *Jaumé and Sykes*, 1999; *Gerstenberg et al.*, 2001] and their spatial organization [*Kagan*, 1991]. These variations can be used for better characterize the seismic hazard in a given region, as well as to infer mechanical properties of the rupture processes. Such mechanical analysis is performed by comparing the statistical patterns of seismicity with those of acoustic emissions at laboratory scale [*Mogi*, 1962; *Scholz*, 1968] or of rupture events in numerical models of rock deformation [see *Main*, 1996, for a review]. *Bethoux et al.* [1998] have applied statistical approaches to the seismicity of the western Alps based on a global database in this belt. Here, we statistically analyze the seismicity of two well-defined geological structures in the internal western Alps in order to test whether these structures exhibit a different mechanical behavior in terms of ductile/brittle deformation and if so, to propose a physical rationale for this difference.

0094-8276/02/2001GL014050$05.00

2. Structural and Tectonic Settings

[3] Within the internal western Alps, historical and instrumental seismicity defines two elongated seismic zones [*Rothé*, 1941; *Grasso et al.*, 1992; *Sue et al.*, 1999] that coincide with major Alpine structures (Figure 1). To the West, the Briançonnais seismic arc (BSA) follows the main Oligocene thrust of internal zones onto external zones of the western Alps (i.e. the so-called ''Crustal Penninic Front'', CPF, *Tricart* [1984]; *Sue et al.* [1999]). To the east, the Piemont seismic arc (PSA) is located on the western edge of a mantle and lower crustal indenter, the Ivrea Body (IB) [*Berkhemer*, 1968; *Paul et al.*, 2001]. From a tectonic point of view, the CPF resulted from thrusting within upper crustal rocks, whereas the IB is a crustal scale indenter which brings mantle and lower crustal rocks in contact with upper crustal rocks. These two main structures are inherited from Oligo-Miocene compressive tectonic phases in the western Alps' history. Recent results of a multidisciplinary analysis of stress and strain indicators, including earthquake focal mechanism [*Sue et al.*, 1999], faulting [*Sue and Tricart*, 2002], and geodesy [*Sue et al.*, 2000], provide evidences for a recent and still active widespread extension in the core of the belt. The seismic activity of the two arcs is identified mainly as normal faulting [*Sue et al.*, 1999]. Most of the hypocenters are located in the 0–20 km range for both arcs (Figure 1). In the BSA zone, the normal faulting is located in the hangingwall of the CPF. Focal mechanism dips (40–60°) agree with the overall dip of the BSA. In the PSA the focal plane dips (40–60°) disagree with the vertical trend of the seismicity, which occurs on the contact zone between the upper crustal rocks and the IB material. Since the seismic activity of BSA and PSA coincides spatially with the inherited crustal structures, BSA and PSA are proposed to map their reactivation under the same contemporary extensional tectonic loading. Here we investigate the statistics of earthquakes for the two seismic arcs (BSA and PSA) in order to constrain the mechanical behavior of the associated structures (CPF and IB).

3. Methods and Data Analysis

[4] We used 1812 earthquakes recorded by permanent alpine seismic networks during the 1989–1997 period. We selected earthquakes according to the following criteria: (i) root means square residual < 1s, (ii) azimuthal gap < 180°, (iii) number of arrival times used for location > 10. We used the same criteria as *Sue et al.* [1999], with the exception of the minimum threshold for magnitude. The two seismic arcs studied here are located in the central part of the seismic networks. To estimate the magnitude

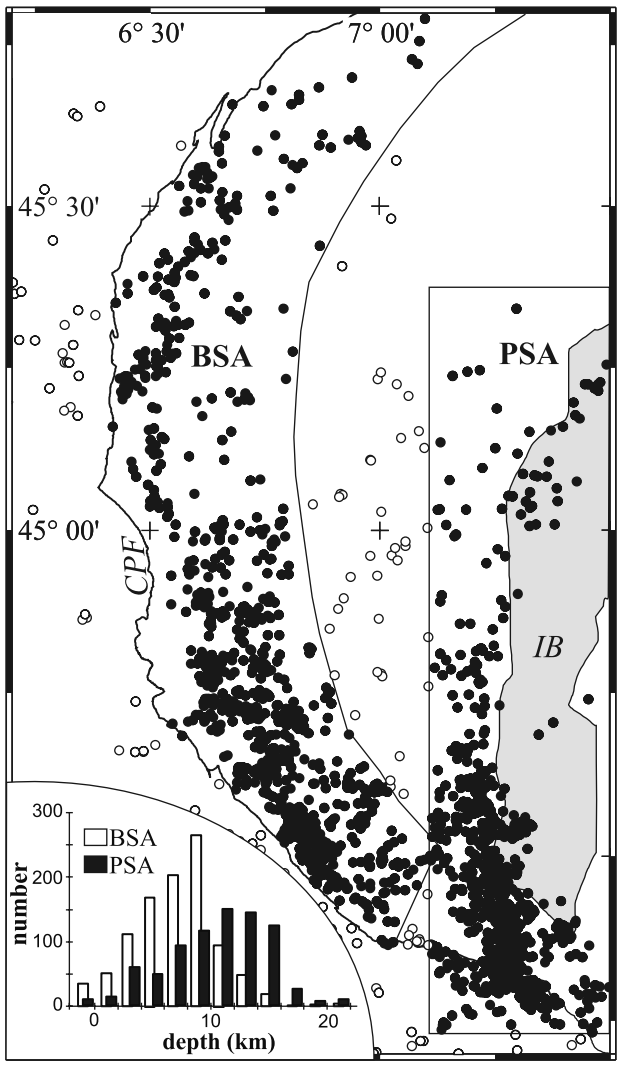

Figure 1. Map of the western Alpine seismicity with the boxes of BSA and PSA defined in the text. Because of its complexity, the western window discards the very southern tip of BSA. Histograms are the depth distribution of BSA (white, 1008 events, average depth 7.2 km) and PSA (black, 804 events, average depth 10.5 km).

order of location uncertainties, *Sue* [1998] measured changes in hypocenter locations induced by changes in the velocity model. When using 1D 3-layers, 1D 12-layers and a 3D model, epicenters and focal depth fall, respectively, within about 1 km and 2 km in distance.

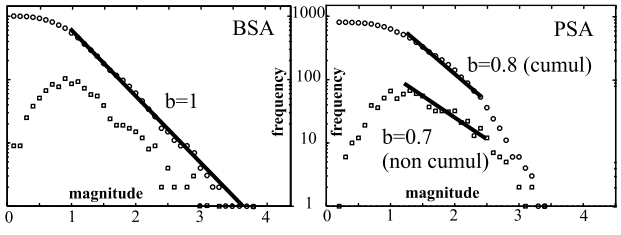

Figure 2. Cumulative (circles) and non-cumulative (squares) energy distributions of BSA (b-value = 1, magnitude range = [1–3.8]) and PSA (b-value = 0.8, magnitude range = [1.2–2.3]). Due to the truncated distribution for PSA, the 0.7 non cumulative b-value is probably a better estimation.

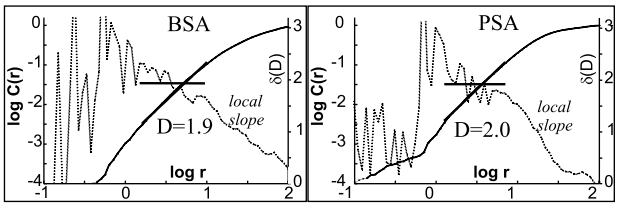

Figure 3. Correlation integral (thick line) and its derivative (dotted line) for BSA (D = 1.9 ± 0.06, distance range = [1.5–9]) and PSA (D = 2.0 ± 0.05, distance range = [1.2–7]).

[5] We define earthquakes relevant to each arc (BSA and PSA) according to the following criteria. For BSA, we used a spatial window of 35 km width eastward of the surface expression of the CPF. For the PSA, we used a rectangular box of 40 * 130 km (Figure 1). We characterized the statistical behavior of the two seismic arcs in the energy domain using the frequency-magnitude distribution of earthquakes (Figure 2). For 1008 earthquakes ranging in magnitude from 0.5 to 3.8, the BSA shows a typical Gutenberg-Richter law (power law distribution of earthquake energies), with a cut-off for low magnitude (Ml < 1). The exponent of the power law distribution (so-called b-value) is close to 1, the value recorded for global earth seismicity [*Gutemberg and Richter*, 1944; *Scholz*, 1990]. The PSA magnitude distribution, for 804 earthquakes with 0.5 < Ml < 3.5, shows a departure from a pure power law distribution. The power law model is reasonably respected over one order of magnitude [1.2–2.3] but there is a fall off for [2.3–3.5] magnitude range. Accordingly, we measured the b-value only in the quite narrow [1.2–2.3] range. We found b = 0.8 using the cumulative distribution, which integrates the second part of the distribution [2.3–3.5], and thus tends to increase the b-value. Therefore the value b = 0.7, measured from the non-cumulative distribution in the same range of magnitudes [1.2–2.3] is probably a better estimation of the PSA b-value.

[6] In order to quantitatively characterize the spatial organization of brittle damage in the two seismic arcs (relatively diffuse or localized), we used the correlation integral method [*Grassberger and Procaccia*, 1983], i.e. we plotted in logarithmic scales the proportion C(r) of pairs of events separated by a distance smaller than r, as a function of r. In ranges where the plot exhibits a straight line, i.e. where $C(r) \sim r^D$, the population can be considered as fractal. The slope D (so-called correlation dimension) is a measure of the degree of clustering of hypocenters and can theoretically range in a 3D space from 3 for a set of hypocenters uniformly distributed at random to 0 for all hypocenters collapsed into one point. The choice of the range on which we measured D was carried out by following the recommendations of *Eneva* [1996]. Accordingly we did not restrict a priori our range of analysis to that inferred from a theoretical formalism [*Nerenberg and Essex*, 1990]. We plotted C(r) on all scales and used the two points slope technique to determine the range where D could be measured most reasonably (Figure 3). Using this technique, we measured D = 2.0 ± 0.05 for PSA in the 1.2–7 km range, and D = 1.9 ± 0.06 for BSA in the 1.5–9 km range. In 2 dimensions (discarding the depth), we obtained D = 1.4 ± 0.04 for PSA and D = 1.38 ± 0.05 for BSA. However, for a given data set, the genuine D-value is affected both by the number of data and the size of the embedding volume. In order to be able to compare the spatial pattern of the two seismic arcs, we computed D-values for 100 sets of the same number of events uniformly distributed at random in the same volume as the real ones. For PSA we used a volume of 130*40*20 km^3 and for BSA an arcuate volume (130° of aperture, 60 < R < 95 km, depth of 20 km), which best fits the BSA's geometry. When comparing synthetic and observed correlation dimension plots, we find (i) a common cut-off for r > 7–9 km; (ii) a cut-off for r < 1–2 km only for observed distributions. The upper cut-off is typical of a finite size effect of the sampled volume, whereas the lower cut-off, close

to 1 km, highlights the location accuracy of earthquakes, as independently estimated by *Sue* [1998]. The D-values deduced from the synthetic catalogues allow us to compare the observed values for the two arcs by their relative distance to their respective synthetic uniform distribution. In the 1–10 km range, the average synthetic D-value for PSA and BSA boxes are 2.8 in 3D (1.8 in 2D). The distances between observed and synthetic populations are therefore 0.8 for PSA and 0.9 for BSA in 3D (0.4 in 2D). On the 3D analysis basis, PSA seismicity is suggested to be relatively more diffuse than BSA seismicity, the two arcs being significantly more clustered than a uniform population.

4. Discussion

[7] We characterized the energy and space statistical distributions of BSA and PSA seismicity, which we propose to analyze in terms of mechanical behavior. For both seismic arcs, we recovered a self-similar organization of seismicity in energy and space domains in a certain scale range. Such self-similarity is typical of earthquake populations and strongly argues for the earth's crust to behave as a dynamic system close to a critical phase transition [*Binney et al.*, 1992; *Bak and Tang*, 1989]. For ruptures initiated in a system, such transition could correspond to the passage from a phase where they tend to die out rapidly (subcritical phase) to a phase where they tend to propagate throughout the system (supercritical phase) [*Main*, 1996]. However, in the western Alps, we also observe differences between the statistical behavior of the two seismic arcs, although they are located a few kilometers from each other. First we try to identify the mechanisms that drive the change from a truncated power law energy distribution for PSA seismicity to a pure power law distribution for BSA seismicity. The truncated PSA energy distribution can correspond to a finite size effect. These effects have been reported at different scales within the earth's crust [*Main*, 1992; *Pacheco et al.*, 1992; *Volant and Grasso*, 1994; *Grasso and Sornette*, 1998]. For PSA and BSA, tectonic arguments do not explain why a finite size effect would affects PSA and not BSA. The truncated PSA energy distribution can also correspond to a genuine subcritical behavior, indicating a finite correlation length in the rupture dynamics of PSA that can be induced by numerous factors. Firstly, in the BSA/PSA case, there is no support for a difference in the driving strain. Secondly, intrinsic properties of the host rocks may lead to such a subcritical behavior of the system, including heterogeneity of rock strength [*Rundle and Klein*, 1993; *Main et al.*, 2000], low permeability [*Henderson and Maillot*, 1997] and low viscosity [*Yoshino*, 1998] of crust-forming rocks, e.g. due to creep mechanisms like pressure solution. In the spatial domain, our analysis shows that the seismicity of the two arcs is non uniform (difference of 0.9 and 0.8 in D-value relative to a uniform distribution for BSA and PSA, resp.), BSA being slightly more localized than PSA.

[8] Although there are numerous parameters that possibly control b and D values, their interpretation was recently proposed and modeled in terms of damage processes in rock mechanics, [*Tang*, 1997; *Zapperi et al.*, 1997; *Amitrano et al.*, 1999; *Wang et al.*, 2000]. The four models reproduce power law distributions of spatial damage with increasing deformation. *Wang et al.* [2000] suggest that the b-value depends on the pre-existing crack length distribution of the material. The *Zapperi et al.* [1997] and *Tang* [1997] models do not allow to reproduce variations in b-value with increasing deformation. *Amitrano et al.* [1999] propose that b and D values depend on a single generic control parameter, the internal friction angle (π), which also determines the shape of the event size distribution (pure or truncated power law) and the kind of macroscopic behavior (ductile-brittle transition). This generic approach allows to rationalize other possible less generic parameter such as heterogeneity (strength or cracks distribution) or confining pressure, that are described in many mechanical experiments. Using this model, π values with both b-value and distribution shapes comparable to our data are 22° and 38° for PSA and BSA, respectively (Figure 4). Using both the shape of the power law distributions and the b and D values, numerical simulations suggest a more brittle behavior for BSA relatively to PSA, driven by a higher internal friction angle. Note that the observed difference in PSA/BSA D-values, which emerges only from 3D-calculation, is smaller than the modeled one.

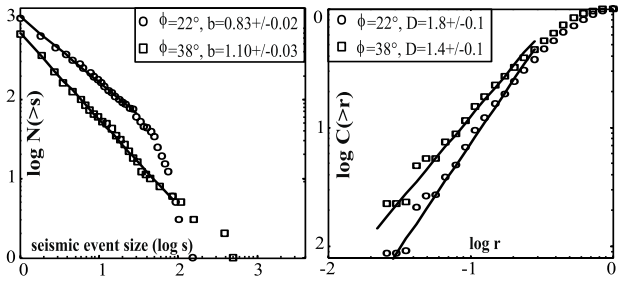

Figure 4. Event size distribution and correlation integral obtained from 2D numerical simulation for $\pi = 22°$ and $\pi = 38°$ [*Amitrano et al.*, 1999]. π is the internal friction angle of the rock mass. The event size s is the number of damaged elements during an avalanche. r is the distance relative to the model size. Although many macroscopic factors control b-value in a given geodynamic system, *Amitrano et al.* [1999] have performed parameters sensibility tests which have shown that both macroscopic behavior, damage spatial distribution and seismic event size distribution are controlled by the single parameter phi. The analysis of the Mohr-Coulomb criterion field around defects revealed that the phi parameter controls the geometry of the interaction between defects and thus control both the spatial distribution of damage (described by D) and the events dynamics (described by b) and the mechanical behavior.

[9] From a tectonic point of view, such differences in b and D values (interpreted as brittle vs. ductile behavior) could be due to: (i) depth, which is correlated to increase in lithostatic/confining pressure. Such an explanation is consistent with independent reports of a decrease of the seismic b-value with earthquakes depth [*Mori and Abercombie*, 1997] and with confining pressure in acoustic emission laboratory experiments [*Amitrano*, 1999]. Following *Mori and Abercombie* [1997], b-value would decrease of about 0.15 between 7 km and 10 km of depth. Thus, the difference of average depth between BSA and PSA could explain an important part of our observations. However, the depth is probably not the single driving process; (ii) material composition, which may lead to a different internal angle of friction. BSA (upper crust material) and PSA (mantle/lower crust material within upper crust material) have indeed a different rock composition; (iii) geometry of inherited damage. Observations of fracture orientations (deduced from earthquake focal mechanisms, *Sue et al.* [1999]), argue for co-operative faulting on BSA. Earthquake focal mechanism dips (40–60°) agree with the overall dip of BSA hypocenters. On the contrary, the PSA seismicity appears as less correlated on the basis of both the discrepancy between vertical trend of seismicity and focal plane dips, and the relatively larger D-value. A more diffuse inherited damage in PSA would induce a lower b-value and a higher D-value. Thus, changes in b and D values would emerge from localized and diffuse inherited damage geometry on BSA and PSA respectively. Our analysis is based on ten years of seismic monitoring. If such behavior is shown to be stationary through time, it would imply a greater probability of large earthquakes for BSA than for PSA.

5. Conclusion

[10] In an attempt to use seismicity to infer mechanical properties of geological objects, we analyzed the statistical distribution

patterns in energy and space domains for two seismic arMcs in the western French-Italian Alps (BSA and PSA). For the two arcs, we found a fall-off for large events for the energy distribution of PSA only, and roughly similar spatial damage. When comparing known structural and tectonic settings for the two arcs, such fall-off for large earthquakes can be identified neither as a finite size effect nor as a difference in driving parameters of the arc dynamics. Damage models of macroscopic rock matrix behavior simulate statistical distributions and exponent that reproduce the observed BSA and PSA distributions. It would imply a change in friction angle value between the two seismic arcs. Globally, the BSA damage appears to be more brittle than the PSA damage. We suggest three possible candidates to drive the changes in apparent internal friction angle between BSA and PSA mechanics of faulting: the earthquake depth, the host rock composition, and the inherited fracturing patterns.

[11] **Acknowledgments.** We thank the Sismalp (Grenoble, France) and IGG (Genova, Italy) groups for making their data available. We are grateful to S. Zapperi and A. Helmstetter for fruitful discussions. We thank K. Verrecchia and M. Burkhard for many improvements they brought to the manuscript, and a reviewer, whose the critical remarks helped to improve this paper. We wish to thank ME. Claudel, O. Sue and ENS Lyon students (1999) for their collaboration in the early stage of this work. This work was supported by Neuchâtel University, the Grenoble Observatory, and the French PGRN program.

References

Amitrano, D., J. R. Grasso, and D. Hantz, From diffuse to localised damage through elastic interaction, *GRL*, *26*, 2109–2112, 1999.

Amitrano, D., Emission acoustique des roches et endommagement: Approche expérimentale et numérique, application à la sismicité minière. *PhD thesis,* UJF Grenoble, France, 1999.

Bak, P., and C. Tang, Earthquakes as a self-organized critical phenomenon, *J. Geophys. Res.*, *94*, 15,635–15,637, 1989.

Berkhemer, H., Topographie des Ivrea-Körpers abgeleitet aus seismischen und gravimetrischen Daten, *Schweiz. Min. Petr. Mit.*, *48*, 235–246, 1968.

Bethoux, N., G. Ouillon, and M. Nicolas, The instrumental seismicity of the Western Alps; spatio-temporal patterns analysed with the wavelet transform, *G. J. I.*, *135*, 177–194, 1998.

Binney, J., N. J. Dowrick, A. J. Fisher, and M. E. Newmann, The theory of critical phenomena. An introduction to the renormalization group, Oxford Univ. Press, 1992.

Eneva, M., Effect of limited data sets in evaluating the scaling properties of spatially distributed data: An example from mining induced seismic activity, *G. J. I.*, *124*, 773–786, 1996.

Gerstenberg, M., S. Wiemer, and D. Giardini, A systematic test of the hypothesis that the b value varies with depth, *GRL*, *28*, 57–60, 2001.

Grassberger, P., and I. Procaccia, Measuring the strangeness of strange attractors, *Physica*, *9*, 189–208, 1983.

Grasso, J. R., F. Guyoton, J. Fréchet, and J. F. Gamond, Triggered earthquakes as stress gauge: Implication for uppercrust behavior in the Grenoble area, France, *P. Appl. Geoph.*, *139*, 579–606, 1992.

Grasso, J. R., and D. Sornette, Testing self-organized criticality by induced seismicity, *J. Geophys. Res.*, *103*, 29,965–29,987, 1998.

Gutemberg, B., and C. Richter, Frequency of earthquakes in California, *Bull. Seismol. Soc. Am.*, *34*, 185–188, 1944.

Henderson, J., and B. Maillot, The influence of fluid flow in fault zones on patterns of seismicity: A numerical investigation, *J. Geophys. Res.*, *102*, 2915–2924, 1997.

Jaumé, S. C., and L. R. Sykes, Evolving toward a critical point: A review of accelerating seismic moment/energy release prior to large and great earthquakes, *P. Appl. Geoph.*, *155*, 279–306, 1999.

Kagan, Y., Fractal dimension of brittle fracture, *J. Nonlinear Sci.*, *1*, 1–16, 1991.

Main, I. G., Earthquake scalling; discussion, *Nature*, *357*, 27–28, 1992.

Main, I. G., Statistical physics, seismogenesis, and seismic hazard, *Rev. Geophys.*, *34*, 433–462, 1996.

Main, I. G., G. O'Brien, and J. R. Henderson, Statistical physics of earthquakes; comparison of distribution exponents for source area and potential energy and the dynamic emergence of log-periodic energy quanta, *J. Geophys. Res.*, *105*(3), 6105–6126, 2000.

Mogi, K., Study of the elastic shocks caused by the fracture of heterogeneous materials and its relation to earthquake phenomena, *Bull. Earthq. Res. Int.*, *40*, 125–173, 1962.

Mori, J., and R. E. Abercombie, Depth dependence of earthquake frequency-magnitude distributions in California: Implication for rupture initiation, *J. Geophys. Res.*, *102*, 15,081–15,090, 1997.

Nerenberg, M. A. H., and C. Essex, Correlation dimension and systematic geometric effects, *Phys. Rev. A*, *42*, 1065–1074, 1990.

Pacheco, J., C. Scholz, and L. Sykes, Changes in frequency-size relationship from small to large earthquake, *Nat.*, *355*, 71–73, 1992.

Paul, A., M. Cattaneo, F. Thouvenot, D. Spallarossa, N. Bethoux, and J. Fréchet, A 3D crustal velocity model of the SW Alps from local earthquake tomography, *JGR*, *106*, 19,367–19,389, 2001.

Rothé, J. P., Les séismes des Alpes françaises en 1938 et la sismicité des Alpes occidentales, *Ann. Inst. Phys. Globe Strasb*, 1–105, 1941.

Rundle, J. B., and W. Klein, Scaling and critical phenomena in a cellular automaton slider-block model for earthquakes, *J. Stat., Phys.*, *72*, 405–413, 1993.

Scholz, C. H., The frequency-magnitude relation of microfracturing in rock and its relation to earthquake, *BSSA.*, *58*, 399–415, 1968.

Scholz, C. H., The mechanics of earthquakes and faulting, Cambridge University Press, 1990.

Sue, C., Dynamique actuelle et récente des Alpes occidentales internes approche structurale et sismologique, *PhD* Grenoble, 1998.

Sue, C., F. Thouvenot, J. Fréchet, and P. Tricart, Earthquake analysis reveals widespread extension in the core of the Western Alps, *J. Geophys. Res.*, *104*, 25,611–25,622, 1999.

Sue, C., and P. Tricart, Widespread post-nappe normal faulting in the internal western Alps: A new constraint on arc dynamics, *J. Geol. Soc. London*, *159*, 61–70, 2002.

Sue, C., J. Martinod, P. Tricart, F. Thouvenot, J. F. Gamond, J. Fréchet, D. Marinier, J. P. Glot, and J. R. Grasso, Active deformation in the inner W. Alps inferred from comparison between 1972-classical and 1996-GPS geodetic surveys, *Tectonophys.*, *320*, 17–29, 2000.

Tang, C. A., Numerical simulation of progressive rock failure and associated seismicity, *Int. J. Rock Mech. Abstr*, *34*, 249–261, 1997.

Tricart, P., From passive margin to continental collision: a tectonic scenario for the Western Alps, *Am. J. Sci.*, *284*, 97–120, 1984.

Volant, P., and J. R. Grasso, The finite extension of fractal geometry and power law distribution of shallow earthquakes: A geomechanical effect, *J. G. R.*, *99*, 21,879–21,889, 1994.

Wang, Y. C., X. C. Yin, F. J. Ke, M. F. Xia, and K. Y. Peng, Numerical simulation of rock failure and earthquake process on mesoscopic scale, *Pageoph*, *157*, 1905–1928, 2000.

Wiemer, S., and M. Wyss, Mapping frequency-magnitude distribution in asperities: An improved technique to calculate recurrence times, *J. Geophy Res*, *102*, 15,115–15,128, 1997.

Yoshino, T., Influence of crustal viscosity on earthquake energy distribution in a viscoelastic pring-block model, *Geophys. Res. Lett.*, *25*(19), 3643–3646, 1998.

Zapperi, S., A. Vespignani, and E. Stanley, Plasticity and avalanche behaviour in microfracturing phenomena, *Nat.*, *388*, 658–660, 1997.

D. Amitrano, LAEGO-EMN, parc Saurupt, 54042 Nancy Cedex, France. (david.amitrano@mines.u-nancy.fr)

J. R. Grasso, LGIT, BP53, 38041 Grenoble Cedex, France. (grasso@lgit.obs.ujf-grenoble.fr)

F. Lahaie, Department Geology, University College, Belfield, Dublin 4, Ireland. (franz.lahaie@ucd.ie)

C. Sue, Geological Institute, Neuchâtel University, r. Argand 11, 2007, Neuchâtel, Switzerland. (christian.sue@unine.ch)